

# A lattice Boltzmann method for thermal nonideal fluids

G. Gonnella<sup>1</sup>, A. Lamura<sup>2</sup>, and V. Sofonea<sup>3</sup>

<sup>1</sup> Dipartimento di Fisica, Università di Bari and Istituto Nazionale di Fisica Nucleare, Sezione di Bari, via Amendola 173, 70126 Bari, Italy

<sup>2</sup> Istituto Applicazioni Calcolo, CNR, via Amendola 122/D, 70126 Bari, Italy

<sup>3</sup> Center for Fundamental and Advanced Technical Research, Romanian Academy, Bd. Mihai Viteazul 24, 300223 Timișoara, Romania

**Abstract.** A Lattice Boltzmann Method for van der Waals fluids with variable temperature is described. Thermo-hydrodynamic equations are correctly reproduced at second order of a Chapman-Enskog expansion. The method is applied to study initial stages of phase separation of a fluid quenched by contact with colder walls. Thermal equilibration is favoured by pressure waves which propagate with the sound velocity.

## 1 Introduction

Heat transport in fluid systems gives rise to a rich phenomenology relevant in many technological applications [1]. The understanding of the behaviour of thermal fluids is often based on numerical studies so that efficient methods of simulations are required.

In recent years Lattice Boltzmann Method (LBM) has been applied to study single, multi-component and complex fluids [2] for different kinds of processes and setup. The method can easily handle complex geometries and is suitable for parallel implementation [3]. The dynamics of the fluid is modelled by Boltzmann equations for a set of distribution functions representing the densities of particles moving along fixed lattice directions. Conservation laws and proper choices of equilibrium distributions in the collision terms ensure that the correct hydrodynamic equations are recovered in the continuum limit.

In this paper we describe a lattice Boltzmann scheme which allows to simulate the thermo-hydrodynamic equations for a van der Waals fluid. In order to describe systems with interfaces, gradient coarse-grained contributions to free energy are also included. The method correctly reproduces in the continuum, at second order of a Chapman-Enskog expansion, the transport equations for a non ideal fluids as recently established by Onuki [4]. Previous LBM for thermal fluids have been so far only set up for ideal fluids [5] or do not consider all terms present in continuum equations [6,7]. We use a finite difference lattice Boltzmann method (FDLBM), where the relationship  $c = \delta s / \delta t$  among the lattice speed  $c$  and the space and time steps  $\delta s$  and  $\delta t$  does no longer hold. FDLBM enable to implement different discretization schemes and this is useful for improving numerical stability and in cases with nonuniform grids or for mixtures with different masses. Moreover, the Prandtl number can be varied independently on the viscosity.

In section II and III a detailed presentation of the method is given. In section IV numerical results are shown for the initial stages of phase separation of a fluid quenched by contact with colder walls at a temperature below the critical value. While in many simulations and theories the temperature jump is assumed instantaneous in all the system [8], here, as it occurs in many realistic situations, the temperature of the bulk does not set immediately at the value of the walls and this can influence the phase separation. We will see that pressure waves created

by thermal contraction near the walls speed up the thermal equilibration of the system. The propagation speed of these waves has been evaluated for different cases.

## 2 General description of the model

In this paper we use the two-dimensional FDLBM with multiple speeds of Watari and Tsutahara [9], which allows the recovery of mass, momentum and energy equations of a fluid with variable temperature. The model involves a set of 33 nondimensionalized velocities  $e_{00} = 0, e_{ki} = [\cos \frac{\pi(i-1)}{4}, \sin \frac{\pi(i-1)}{4}]c_k$  ( $k = 1, \dots, 4, i = 1, \dots, 8$ ) where the values of the speeds  $c_k \in \{1.0, 1.92, 2.99, 4.49\}$  were determined in [9] to ensure the stability of this model within the temperature range  $0.4 \leq \theta \leq 1.6$ . The corresponding distribution functions  $f_{00} = f_{00}(\mathbf{x}, t)$ ,  $f_{ki} = f_{ki}(\mathbf{x}, t)$  are defined in the nodes  $\mathbf{x}$  of a square lattice and evolve according to

$$\partial_t f_{ki} + \mathbf{e}_{ki} \cdot \nabla f_{ki} = -\frac{1}{\tau}[f_{ki} - f_{ki}^{eq}] + I_{ki} \quad (1)$$

where the relaxation time  $\tau$  is constant and the term  $I_{ki}$  accounts for interparticle forces (more details related to this term will be introduced in the next section).

The local fluid density  $n$ , velocity  $\mathbf{u}$ , and temperature  $\theta$  are determined from the distribution functions  $f_{ki}$  as follows [9]:

$$n = \sum_{ki} f_{ki} \quad (2)$$

$$nu_\alpha = \sum_{ki} f_{ki} e_{ki\alpha} \quad (3)$$

$$n \left( \theta + \frac{u^2}{2} \right) = \frac{1}{2} \sum_{ki} f_{ki} c_k^2. \quad (4)$$

The equilibrium distribution functions which appear in Eqs. (1),

$$f_{ki}^{eq} = f_{ki}^{eq}(\mathbf{x}, t) = n F_k s_{ki} \quad (5)$$

are expressed using the series expansion  $s_{ki} = s_{ki}(\theta, \mathbf{u})$  up to fourth order [9] with respect to the Cartesian components  $u_\alpha$  ( $\alpha = 1, 2$ ) of the fluid velocity (summation over repeated Greek indices is understood):

$$\begin{aligned} s_{ki} = & \left( 1 - \frac{u^2}{2\theta} + \frac{u^4}{8\theta^2} \right) + \frac{1}{\theta} \left( 1 - \frac{u^2}{2\theta} \right) e_{ki\xi} u_\xi + \frac{1}{2\theta^2} \left( 1 - \frac{u^2}{2\theta} \right) e_{ki\xi} e_{ki\eta} u_\xi u_\eta \\ & + \frac{1}{6\theta^3} e_{ki\xi} e_{ki\eta} e_{ki\zeta} u_\xi u_\eta u_\zeta + \frac{1}{24\theta^4} e_{ki\xi} e_{ki\eta} e_{ki\zeta} e_{ki\chi} u_\xi u_\eta u_\zeta u_\chi. \end{aligned} \quad (6)$$

The weight factors  $F_k = F_k(\theta)$  in Eq. (5) depend on the local temperature  $\theta = \theta(\mathbf{x}, t)$  and the speeds  $c_k$ ,  $k = 1, \dots, 4$ :

$$\begin{aligned} F_k = & \frac{1}{c_k^2 (c_k^2 - c_{\{k+1\}}^2) (c_k^2 - c_{\{k+2\}}^2) (c_k^2 - c_{\{k+3\}}^2)} \\ & \times [48\theta^4 - 6(c_{\{k+1\}}^2 + c_{\{k+2\}}^2 + c_{\{k+3\}}^2)\theta^3 + (c_{\{k+1\}}^2 c_{\{k+2\}}^2 + c_{\{k+2\}}^2 c_{\{k+3\}}^2 \\ & + c_{\{k+3\}}^2 c_{\{k+1\}}^2)\theta^2 - c_{\{k+1\}}^2 c_{\{k+2\}}^2 c_{\{k+3\}}^2 \theta/4] \end{aligned} \quad (7)$$

$$F_0 = 1 - 8(F_1 + F_2 + F_3 + F_4). \quad (8)$$

Here we used the notation  $\{k+l\} = k+l$  ( $k+l \leq 4$ ),  $k+l-4$  ( $k+l > 4$ ) for  $l = 1, 2, 3$ .

Since the nondimensionalized speeds  $c_k$  of the thermal LB model are no longer related to the lattice spacing  $\delta s$  and the time step  $\delta t$ , as in the standard (collision - streaming) LB models

[3,10], finite difference schemes need to be used to evolve the distribution functions in each lattice node [9,11]. To reduce numerical errors, the Monitorized Central Difference (MCD) flux limiter finite difference scheme [12–14] is used in this paper. This scheme is briefly outlined.

If  $f_{ki,j}^n = f_{ki}(\mathbf{x}_j, t)$  is the value of the distribution function  $f_{ki}$  at time  $t$  in the node  $\mathbf{x}_j$  on the characteristic line along the direction  $i$ , the updated value  $f_{ki,j}^{n+1} = f_{ki}(\mathbf{x}_j, t + \delta t)$  of the distribution function  $f_{ki}$  at time  $t + \delta t$  in the node  $\mathbf{x}_j$  is computed using two fluxes

$$f_{ki,j}^{n+1} = f_{ki,j}^n - \frac{c_k \delta t}{A_i \delta s} [F_{ki,j+1/2}^n - F_{ki,j-1/2}^n] - \frac{\delta t}{\tau} [f_{ki}^n - f_{ki}^{eq,n}] + \delta t I_{ki}^n \quad (9)$$

where  $A_i = 1 (i \in \{1, 3, 5, 7\}), \sqrt{2} (i \in \{2, 4, 6, 8\})$  and the outgoing and incoming fluxes in node  $j$  along the direction  $i$  are

$$F_{ki,j+1/2}^n = f_{ki,j}^n + \frac{1}{2} \left( 1 - \frac{c_k \delta t}{A_i \delta s} \right) [f_{ki,j+1}^n - f_{ki,j}^n] \Psi(\Theta_{ki,j}^n) \quad (10)$$

$$F_{ki,j-1/2}^n = F_{ki,(j-1)+1/2}^n. \quad (11)$$

The MCD flux limiter is given by [12,14]

$$\Psi(\Theta_{ki,j}^n) = \begin{cases} 0, & \Theta_{ki,j}^n \leq 0 \\ 2\Theta_{ki,j}^n, & 0 \leq \Theta_{ki,j}^n \leq \frac{1}{3} \\ (1 + \Theta_{ki,j}^n)/2, & \frac{1}{3} \leq \Theta_{ki,j}^n \leq 3 \\ 2, & 3 \leq \Theta_{ki,j}^n \end{cases} \quad (12)$$

where  $\Theta_{ki,j}^n = \frac{f_{ki,j}^n - f_{ki,j-1}^n}{f_{ki,j+1}^n - f_{ki,j}^n}$  is the smoothness function.

In our simulations, the two-dimensional fluid system was placed between two parallel walls at rest ( $\mathbf{u}_w = 0$ ). Both walls have the constant temperature  $\theta_w$  and diffuse reflection boundary conditions [15] were used in order to achieve heat exchange with the fluid. Since the fluid density may vary along the walls, the implementation of the boundary conditions allows the distribution functions, whose velocities point to the wall in the normal direction, to mix separately from the distribution functions with velocities orientated along the diagonals of the square lattice. This procedure is explained in Fig. 1, which refers to the left wall (periodic boundary conditions are used in the vertical direction). The wall is located half lattice spacing between the ghost nodes and the fluid nodes. The black squares ( $j = 1/2, l$ ) and ( $j = 1/2, l + 1/2$ ),  $l = 0, 1, \dots$ , denote the mixing points on the wall. The corresponding (unknown) values of the particle number density are  $n_w^{1/2,l}$  and  $n_w^{1/2,l+1/2}$ , respectively. Because of particle-wall interactions, the distribution function of fluid particles reflected by the walls becomes Maxwellian. The values of the distribution functions  $f_{k1}^{0,l}, f_{k2}^{0,l}$  and  $f_{k8}^{0,l+1}$ , ( $l = 0, 1, \dots$ ), defined in the ghost nodes outside the left wall need to be computed in order to update the distribution functions in the lattice nodes located near the wall. For these nodes, the MCD scheme is reduced to the first order upwind scheme by setting  $\Psi(\Theta_{ki,j}^n) = 0$ .

Following the discretization of the velocity space, in the LB model the Maxwellian distribution function is replaced by the set of equilibrium distribution functions, Eq. (5), and the distribution functions of reflected particles may be calculated in wall nodes using an interpolation procedure. This gives ( $k = 1, \dots, 4$ )

$$\frac{f_{k1}^{0,l+1} + f_{k1}^{1,l+1}}{F_k(\theta_w) s_{k1}(\theta_w, \mathbf{u}_w)} = 2n_w^{1/2,l} \quad (13)$$

$$\frac{f_{k2}^{0,l} + f_{k2}^{1,l+1}}{F_k(\theta_w) s_{k2}(\theta_w, \mathbf{u}_w)} = \frac{f_{k8}^{0,l+1} + f_{k8}^{1,l}}{F_k(\theta_w) s_{k8}(\theta_w, \mathbf{u}_w)} = 2n_w^{1/2,l+1/2}. \quad (14)$$

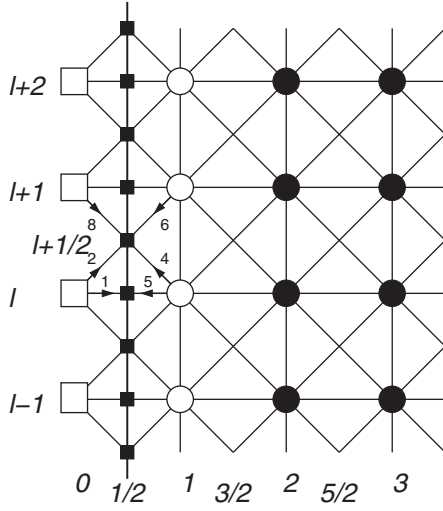


**Fig. 1.** Diffuse reflection boundary conditions:  $\square$  - ghost nodes,  $\circ$  - boundary nodes,  $\bullet$  - bulk nodes,  $\blacksquare$  - wall points where the distribution functions  $f_{ki}$  ( $i = 1, 2, 8$ ) follow the Maxwellian distribution law.

Eqs. (13)–(14), and the requirement that there is no mass flux perpendicular to the wall in the mixing nodes, that is

$$\sum_k c_k f_{k5}^{1,l} = \sum_k c_k f_{k1}^{0,l} \quad (15)$$

$$\sum_k c_k [f_{k4}^{1,l} + f_{k6}^{1,l+1}] = \sum_k c_k [f_{k2}^{0,l} + f_{k8}^{0,l+1}], \quad (16)$$

may be solved to get the values of the distribution functions in the ghost nodes  $(0, l)$  and  $(0, l+1)$  after each time step. Similar relations may be used to compute the values of the corresponding distribution functions in the ghost nodes outside the right wall.

### 3 Force term and the conservation equations of the van der Waals fluid

The extra term  $I_{ki}$  in Eq. (1) takes into account inter-particle forces. Its structure is inspired by the one used by Klimontovich [16] in kinetic theories for nonideal gases

$$I_{ki} = -[A + B_\alpha (e_{ki\alpha} - u_\alpha) + (C + C_q)(e_{ki\alpha} - u_\alpha)^2] f_{ki}^{eq}. \quad (17)$$

$I_{ki}$  is introduced to recover mass, momentum, and energy equations [4]

$$\partial_t n = -\partial_\alpha (n u_\alpha) \quad (18)$$

$$\partial_t (n u_\alpha) = -\partial_\beta (n u_\alpha u_\beta) - \partial_\beta (\Pi_{\alpha\beta} - \sigma_{\alpha\beta}) \quad (19)$$

$$\partial_t e_T = -\partial_\alpha [e_T u_\alpha + (\Pi_{\alpha\beta} - \sigma_{\alpha\beta}) u_\beta] + \partial_\alpha (\kappa_T \partial_\alpha T) \quad (20)$$

for a van der Waals fluid with free-energy

$$F = \int d\mathbf{x} \left[ n\theta \left[ \ln \left( \frac{3n}{3-n} \right) \right] - \frac{9}{8} n^2 + \frac{M}{2} (\nabla n)^2 \right]. \quad (21)$$

$\Pi_{\alpha\beta} = p^w \delta_{\alpha\beta} + \Lambda_{\alpha\beta}$  is the non-viscous stress;  $p^w = \frac{3n\theta}{3-n} - \frac{9}{8} n^2$  is the pressure for a homogeneous system with critical point at  $\theta_c = n_c = 1$ , and  $\Lambda_{\alpha\beta} = M \partial_\alpha n \partial_\beta n - M \left( n \nabla^2 n + \frac{|\nabla n|^2}{2} \right) \delta_{\alpha\beta} - \left( n \theta \partial_\gamma n \partial_\gamma \left( \frac{M}{\theta} \right) \right) \delta_{\alpha\beta}$  is the contribution to the pressure tensor depending on density gradients.

$\sigma_{\alpha\beta} = \eta(\partial_\alpha u_\beta + \partial_\beta u_\alpha - \partial_\gamma u_\gamma \delta_{\alpha\beta}) + \zeta \partial_\gamma u_\gamma \delta_{\alpha\beta}$  is the dissipative stress tensor with shear and bulk viscosities  $\eta$  and  $\zeta$  [17]. The total energy density is  $e_T = n\theta - \frac{9}{8}n^2 + K \frac{|\nabla n|^2}{2} + n \frac{u^2}{2}$ , and the expression  $M = K + H\theta$  ( $K$  and  $H$  constants) allows a dependence of the surface tension on temperature.

$I_{ki}$  gives contributions to the mass, momentum, and energy equations which are

$$\sum_{ki} I_{ki} = A + 2(C + C_q)\theta, \quad (22)$$

$$\sum_{ki} I_{ki} e_{ki\alpha} = -\{nu_\alpha[A + 2(C + C_q)\theta] + n\theta B_\alpha\}, \quad (23)$$

$$\frac{1}{2} \sum_{ki} I_{ki} c_k^2 = -\left\{n \left(\theta + \frac{u^2}{2}\right) [A + 2(C + C_q)\theta] + 2n\theta^2(C + C_q) + n\theta B_\alpha u_\alpha\right\}, \quad (24)$$

respectively. By using a Chapman-Enskog expansion with respect to the Knudsen number  $Kn = c_1\tau/L\delta s$  [3] the coefficients in (17) are set in order to recover Eqs. (18)–(20) by using Eqs. (22)–(24) which give the nonideal contributions.

From the conservation laws and the structure of lattice vectors  $\{\mathbf{e}_{ki}\}$ , it comes out that

$$A = -2(C + C_q)\theta \quad (25)$$

$$B_\alpha = \frac{1}{n\theta} [\partial_\alpha(p^w - n\theta) + \partial_\beta \Lambda_{\alpha\beta} - \partial_\alpha(\zeta \partial_\gamma u_\gamma)] \quad (26)$$

$$C = \frac{1}{2n\theta^2} \left\{ (p^w - n\theta) \partial_\gamma u_\gamma + \Lambda_{\alpha\beta} \partial_\alpha u_\beta - (\zeta \partial_\gamma u_\gamma) \partial_\alpha u_\alpha + \frac{9}{8} n^2 \partial_\gamma u_\gamma \right. \\ \left. + K \left[ -\frac{1}{2} (\partial_\gamma n) (\partial_\gamma n) (\partial_\alpha u_\alpha) - n (\partial_\gamma n) (\partial_\gamma \partial_\alpha u_\alpha) - (\partial_\gamma n) (\partial_\gamma u_\alpha) (\partial_\alpha n) \right] \right\} \quad (27)$$

$$C_q = \frac{1}{2n\theta^2} \partial_\alpha [2qn\theta (\partial_\alpha \theta)]. \quad (28)$$

We stress that Eqs. (18)–(20) are obtained at the second order in  $Kn$  without extra spurious terms. The term  $C_q$  allows to tune the heat conductivity  $\kappa_T$  independently from the dynamic viscosity  $\eta$ . Indeed, we get  $\eta = n\theta\tau$ ,  $\kappa_T = 2n\theta(\tau - q)$  so that the Prandtl number  $Pr = \eta/\kappa_T = \frac{\tau}{2(\tau - q)}$  can be varied by changing the parameter  $q$  keeping  $\tau$  fixed.

When comparing the above introduced FDLBM to other LBM models for thermal non-ideal fluids [6], one should point that, although FDLBM needs more computing resources, all observable fields (density, velocity, temperature) obey the correct continuum equations and are directly derived in our model from the same distribution function, as in standard kinetic theory.

## 4 Results

We studied the initial stages of phase separation of a van der Waals fluid, initially at  $\theta > \theta_c$  with density  $n$  at each lattice node randomly chosen in the interval  $[1.042 - 0.104; 1.042 + 0.104]$ , put in contact with colder walls at  $\theta_W < \theta_c$ . The value  $n = 1.042$  would give symmetric phase separation for an isothermal process with fully periodic boundaries. We used a lattice of size  $L = 512$  with  $\delta s = 1/256$ ,  $\delta t = 10^{-5}$ ,  $K = 10^{-6}$ ,  $H = 0$ , and different values of  $\tau$  and  $q$ . Thermal contraction close to the walls produces a cooling of the system and generates pressure waves which propagate from the walls towards the center of the system. After they come in contact, the waves separate generating a lower pressure between them. The two waves are later reflected from the walls. This phenomenon, also known as piston effect, thermalizes the system much faster than if only due to diffusion. This means that the bulk temperature becomes very soon homogeneous with only a jump close to the walls. In a previous paper it was shown how this mechanism acts during phase separation [18], confirming the picture discussed in Ref. [1].

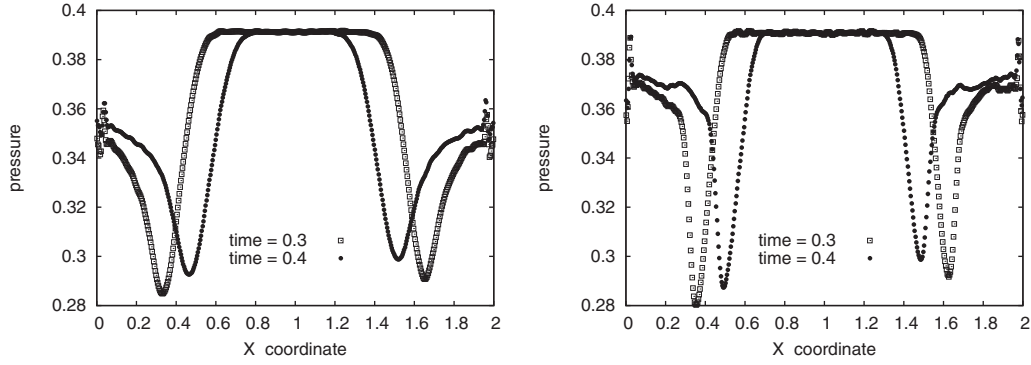


**Fig. 2.** Pressure waves at two times in the cases  $\tau = 0.001$ ,  $\theta_W = 0.90$ , and  $q = -0.004$  (left), 0 (right).

**Table 1.** Propagation speed  $c_p$  for different parameters, compared with the speed of sound  $c_s$ .

$\Theta_W$	$\tau$	$q$	$c_p$	$c_s$
0.95	0.001	-0.004	1.40	1.38
0.90	0.001	-0.004	1.37	1.37
0.85	0.001	-0.004	1.29	1.36
0.90	0.001	-0.004	1.37	1.37
0.90	0.001	0	1.40	1.37
0.90	0.002	0	1.40	1.37

Here we measure the propagation speed of pressure waves acting at initial times of phase separation. We considered different values for the wall temperature ( $\theta_W = 0.85, 0.90, 0.95$ ), viscosity ( $\tau = 0.001, 0.002$ ) and heat conductivity ( $q = -0.004, 0$ ). In Fig. 2 we show the pressure profiles at two consecutive times for the case with  $\theta_W = 0.90$ ,  $\tau = 0.001$ , and  $q = -0.004, 0$ . The slight right-left asymmetry in the profiles is due to the random initial configuration. By measuring the distance  $s_d$  travelled by the minima of waves in a fixed time interval  $t_d$ , we could estimate the propagation speed as  $c_p = s_d/t_d$ . Results are summarized in Table 1 where they are compared with the speed of sound  $c_s$  which is  $\sqrt{2\theta}$  in our model. In order to estimate  $c_s$  we then need to know  $\theta$ . Since the temperature is not constant in the system at initial times due to the quench,  $\theta$  was taken to be the average one in the system over the distance  $s_d$ . We see that by decreasing the wall temperature, the system has a lower bulk temperature which reduces the speed of sound. This trend is also observed in  $c_p$ . When the heat conductivity is increased ( $q$  reduced), the system quenches more rapidly and this produces a decrease in  $c_p$ . Finally, we note that no appreciable effect can be seen by changing the viscosity. Our result  $c_p \simeq c_s$  is in agreement with the findings for supercritical fluids under zero gravity [19].

## 5 Conclusions

We presented a LBM based on a finite difference scheme which can be applied to study the dynamics of a van der Waals fluid. As a numerical application, we considered a quenching process and found that the thermal equilibration is greatly speed-up by pressure waves propagating from the colder regions of the fluid close to the external walls. The velocity of the waves is close to the expected value for the sound speed.

We acknowledge support by GAR 334 (2005-2006) and INFN for a grant at CINECA.

## References

1. A. Onuki, *Phase Transition Dynamics* (Cambridge University Press, Cambridge, 2002)
2. J.M. Yeomans, *Ann. Rev. Comput. Phys.* **VII**, 61 (2000)
3. S. Succi, *The Lattice Boltzmann Equation for Fluid Dynamics and Beyond* (Clarendon Press, Oxford, 2001)
4. A. Onuki, *Phys. Rev. Lett.* **94**, 054501 (2005); *Phys. Rev. E* **75**, 036304 (2007)
5. F.J. Alexander, S. Chen, J.D. Sterling, *Phys. Rev. E* **47**, R2249 (1993); C. Teixeira, H. Chen, D.M. Freed, *Comp. Phys. Comm.* **129**, 207 (2000)
6. B.J. Palmer, D.R. Rector, *Phys. Rev. E* **61**, 5295 (2000); T. Ihle, D.M. Kroll, *Comp. Phys. Comm.* **129**, 1 (2000); R. Zhang, H. Chen, *Phys. Rev. E* **67**, 066711 (2003)
7. T. Seta, K. Kono, S. Chen, *Int. J. Mod. Phys. B* **17**, 169 (2003)
8. See, e.g., A.J. Bray, *Adv. Phys.* **43**, 357 (1994)
9. M. Watari, M. Tsutahara, *Phys. Rev. E* **67**, 036306 (2003)
10. D.A. Wolf-Gladrow, *Lattice Gas Cellular Automata and Lattice Boltzmann Models* (Springer, Berlin, 2000)
11. V. Sofonea, R.F. Sekerka, *Phys. Rev. E* **71**, 066709 (2005)
12. R.J. LeVeque, *Numerical Methods for Conservation Laws* (Birkhäuser, Basel, 1992)
13. E.F. Toro, *Riemann Solvers and Numerical Methods for Fluid Dynamics*, Second Edition (Springer, Berlin, 1999)
14. V. Sofonea, A. Lamura, G. Gonnella, A. Cristea, *Phys. Rev. E* **70**, 046702 (2004); A. Cristea, V. Sofonea, *Cent. Eur. J. Phys* **2**, 382 (2004)
15. S. Ansumali, I.V. Karlin, *Phys. Rev. E* **66**, 026311 (2002); V. Sofonea, *Europhys. Lett.* **76**, 829 (2006); V. Sofonea, *Phys. Rev. E* **74**, 056705 (2006)
16. Y.L. Klimontovich, *Kinetic Theory of Nonideal Gases and Nonideal Plasmas* (Pergamon Press, Oxford, 1982)
17. L.D. Landau, E.M. Lifshitz, *Fluid Mechanics* (Butterworth-Heinemann, Oxford, 1987)
18. G. Gonnella, A. Lamura, V. Sofonea, *Phys. Rev. E* **76**, 036703 (2007)
19. B. Zappoli, D. Bailly, Y. Garrabos, B. Le Neindre, P. Guenon, D. Beysens, *Phys. Rev. A* **41**, 2264 (1990)